A R C H I V E S O F M E T A L L U R G Y A N D M A T E R I A L S
Volume 55 2010 Issue 1

M. LACHOWICZ*, W. DUDZIŃSKI*

NON-EQUILIBRIUM DECOMPOSITION OF MC CARBIDES IN SUPERALLOY INCONEL 713C MELTED WITH WELDING TECHNIQUES

NIERÓWNOWAGOWY ROZPAD WĘGLIKÓW MC W STOPIE INCONEL 713C PRZETAPIANYM TECHNIKAMI SPAWALNICZYMI

In the paper, results of metallographic examination of microstructural changes in superalloy Inconel 713C subject to melting with electron beam or TIG welding followed by thermal treatment are presented. The thermal treatment operations were carried out in 3 time-temperature variants. Within fusion zones, welds and padding welds, (NbTi)C carbides were found in interdendritic areas. Locally, $M_{23}C_6$ or M_6C carbides were present in fusion zones and heat-affected zones. In the matrix of austenite γ and intermetallic phase γ' (Ni_3AlTi), eutectic mixture ($\gamma - \gamma$')-M_xC_y was observed. During fusion and welding, decomposition of γ' phase and (NbTi)C carbides can be caused by the phenomenon of non-equilibrium melting (constitutional liquation). This phenomenon occurs during rapid heating of the alloy. It was found that, during thermal treatment of joints, a different non-carbide phase was created and the eutectic mixture ($\gamma - \gamma$')-M_xC_y was present locally. The thermal treatment did not result in homogenisation of structure and coagulation of carbides, but in decomposition of the carbides. The examination results indicate that decomposition of the (NbTi)C carbides can proceed through the stages of originating the non-equilibrium eutectic mixture ($\gamma - \gamma$')-M_xC_y or the phase $Ni_3(AlTi)C$, followed by creating the supersaturated γ and γ' phases.

Keywords: superalloy, welding, Inconel 713C, carbide (NbTi)C, heat-treatment

W artykule przedstawiono wyniki badań metalograficznych charakteryzujące zmiany mikrostrukturalne w superstopie Inconel 713C, który poddano przetopieniu wiązką elektronów lub metodą TIG, a następnie obróbce cieplnej. Zabiegi obróbki cieplnej prowadzono według 3 wariantów czasowo-temperaturowych. W strefach przetopienia, spoinach i napoinach stwierdzono występowanie w obszarach międzydendrytycznych węglików (NbTi)C. Lokalnie w strefach przetopienia i strefach wpływu ciepła występowały węgliki $M_{23}C_6$ lub M_6C. W osnowie austenitu γ i fazy międzymetalicznej γ' (Ni_3AlTi) wielokrotnie obserwowano mieszaniny eutektyczne ($\gamma - \gamma$')-M_xC_y. W trakcie przetapiania oraz spawania rozpad fazy γ' oraz węglików (NbTi)C może być powodowany zjawiskiem nierównowagowego stapiania określanym również constitutional liquation. Zjawisko występuje podczas gwałtownego nagrzewania stopu. W trakcie obróbki cieplnej stref przetopionych w miejscach występowania węglików (NbTi)C stwierdzono tworzenie się odmiennej fazy niewęglikowej oraz lokalne występowanie eutektyk ($\gamma - \gamma$')-M_xC_y. Obróbka cieplna prowadzona według zadanych parametrów nie powodowała ujednorodnienia struktury oraz koagulacji węglików, lecz ich zanik. W wyniku badań stwierdzono, że rozpad węglików (NbTi)C może przebiegać poprzez tworzenie nierównowagowej eutektyki ($\gamma - \gamma$')-M_xC_y lub fazy $Ni_3(AlTi)C$, a następnie utworzenie przesyconych faz γ i γ'.

1. Introduction

An important element of precipitation hardening of nickel-based superalloys and their creep strength are carbides. In the superalloys, this is most often the carbides type MC, M_6C, $M_{23}C_6$ and M_7C_3. Morphology and arrangement of carbides play an important role in the hardening process. Carbides precipitate on grain boundaries and inside austenite grains, as well as in interdendritic zones, most frequently solidifying directly from liquid [1-12,13,14]. Thanks to stability at high temperature, the most advantageous are simple carbides type MC with A1 structure. In simple carbides, there are often two or more elements, e.g. (Nb,Ti,Mo)C. This reduces durability of the carbides and favours their decomposition at operation or heat-treatment temperatures [1,3]. The carbides NbC, most often occurring in nickel-based superalloys, acc. to [15] can be stable even to 3600 °C and the carbide Nb_2C to 2335 °C. According to [1], the carbides NbC are subject to decomposition only during long heating at temperatures over 1180 °C.

The related references mention reactions transform-

* WROCLAW UNIVERSITY OF TECHNOLOGY, INSTITUTE OF MATERIALS SCIENCE AND APPLIED MECHANICS, 50-370 WROCLAW, 25 SMOLUCHOWSKIEGO STR., POLAND

ing single carbides MC to complex carbides type $M_{23}C_6$ and M_6C, with participation of the elements coming from the solid solution γ [1,5,12,16]. An exemplary decomposition reaction is as follows:

$MC + \gamma = M_{23}C_6$ or $M_6C + \gamma'$

$(Nb,Mo,Ti)C + (Ni,Cr,Al,Ti) = Cr_{21}(NbMo)_2C_6$ or $(CrNbMo)_6C + Ni_3(AlTi)$

Complex carbides $M_{23}C_6$ and M_6C are less stable than carbides MC and can create large precipitates and colonies. The carbides $M_{23}C_6$ can contain also such elements like Co, W, Ni and Fe. The carbides M_6C contain higher percentage of molybdenum. In addition, they can contain also Co and Ni, and have the general formula $(Ni,Co,W)_3Mo_3C$. Both the carbides $M_{23}C_6$ and M_6C can precipitate or melt at temperatures from 800 to 1000 °C, i.e. during heat treatment or welding [1,5,11].

2. Phases present in microstructure of welds and in HAZ

In the authors' research on weldability of the nickel superalloy Inconel 713C, precipitates of the carbides MC, $M_{23}C_6$ and M_6C were observed in fusion zone (FZ), weld and heat-affected zone (HAZ). In the base material (BM), welds, both FZs and HAZ, it was mainly the carbides type (NbTi)C that happened and arose. Locally, the carbides $M_{23}C_6$ and M_6C were observed, to which the formulae $(Cr,Mo)_{23}C_6$ and Cr_3Mo_3C could be ascribed [16-18]. An exemplary microstructure with carbide precipitates in BM, HAZ and FZ is shown in Fig. 1.

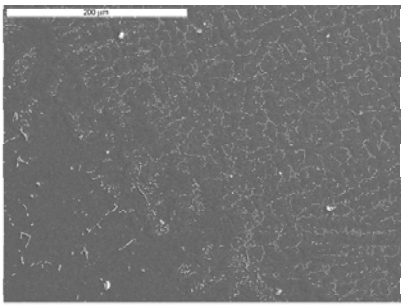

Fig. 1. Changed morphology of carbides in HAZ. Visible precipitates of primary carbides in HAZ and resolidification carbides in FZ. Etched with ML3. SEM

During observations of primary carbides and resolidification (RS) carbides in the welds and HAZ, carbides of highly developed shapes were observed, occurring together with the areas of the eutectic mixture $\gamma - \gamma'$. An exemplary morphology of these carbides is shown in Fig. 2.

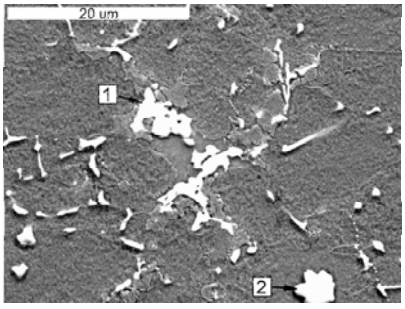

Fig. 2. Developed inclusions of $(\gamma - \gamma')$-(M_xC_y) eutectic in the padding weld. Longitudinal microsection. Etched with ML3. SEM

The averaged concentrations of elements in the precipitate marked "1" in Fig. 2 are given in Table 1 (in atomic percentages):

TABLE 1

Chemical microanalyses of points 1 and 2 in Fig. 2 in at%

Point	Al	Ti	Cr	Fe	Ni	Nb	Mo	Si
1	2.34	1.56	20.57	1.27	44.13	8.92	13.22	7.97
2	–	28.67	–	–	–	71.33	–	–

On the ground of microanalysis only it could be said that the analysed precipitate is a complex carbide, probably type $M_{23}C_6$ $(Cr,Mo,Nb,Si)_{23}C_6$. High nickel content, however, can indicate that the precipitate is very thin and the analysis is influenced by the matrix.

In this precipitate, however, 7 % of silicon was also found. Silicon content in Inconel 713C is below 0.5 %, but it can segregate to niobium carbides and create the low melting compound NbSi. The carbides (NbTi)C and the compound NbSi also show a tendency to create subsequent low melting eutectic mixtures with the solid solution γ. Such eutectics were found e.g. in austenitic steels. In the precipitate marked "2" in Fig. 2, niobium and titanium was found, which indicates the carbide (NbTi)C. The averaged concentrations of elements in the precipitate marked "2" in Fig. 2 are given in Table 1 (in atomic percentages).

Presence of carbides together with the eutectic mix-

ture $\gamma - \gamma$' can evidence that the analysed area includes a complex eutectic mixture ($\gamma - \gamma$')-(M_xC_y). Presence of eutectic mixture in the welds and FZ is related to segregation of components before the solidification front. The eutectic $\gamma - \gamma$' in non-equilibrium conditions is created at 1385 °C. The eutectic mixture γ-(γ+NbC) in Inconel 625 is created at 1350 °C. Because of similar solidification temperatures, creation of one eutectic mixture ($\gamma - \gamma$')-(NbC) is possible. An additional portion of titanium in the carbide NbC and influence of silicon can reduce solidification temperature of the eutectic mixture [19-21].

According to Ojo [22-25], the $\gamma - \gamma$' eutectic reaction in Inconel 738 runs at ca. 1180 °C or even lower temperature, which is related to heating speed. Lowering the real eutectic temperature with respect to the equilibrium system results in non-equilibrium decomposition of γ' particles during welding. A similar phenomenon occurs on the interface carbides-matrix. In literature, the mechanism of melting the phase boundary is called "non-equilibrium melting" or "constitutional liquation" [22-27]. In superalloys, the temperature range in that the eutectic mixture occurs is not exactly recognised. However, both the results of Ojo and his co-workers and the own author's results indicate that temperature of 1180 °C can be the real $\gamma - \gamma$' eutectic temperature. At the same time, the carbide eutectic MC-γ-γ' can arise at an approximate temperature already.

In fusion zones, the resolidification carbides were often observed, with blurred, broadened carbide-matrix boundaries. As various etching techniques proved, this is not formed during preparation of the polished sections but results from the presence of a layer of another phase on the carbides. Exemplary precipitates of the RS carbides are shown in Fig. 2. The carbides in FZ solidify directly from liquid, so concentration of niobium should increase in their vicinity. Rapid cooling would favour restricting the diffusion processes and increasing supersaturation of the phase γ' with niobium. Therefore, solidification temperature of this phase [Ni_3(Al,Ti,Nb)] can be higher in the carbide-containing areas. Therefore, the (NbTi)C carbides can precipitate from supersaturated liquid together with the phase γ'. So, solidification of the eutectic mixture MC-γ-γ' is also possible. The γ' phase can also nucleate on the carbides precipitated before.

The average concentrations of the elements determined for a few largest carbides shown in Fig. 3 were 19.59 wt% Ti, 66.76 wt% Nb, 5.24 wt% Cr and 8.41 wt% Ni.

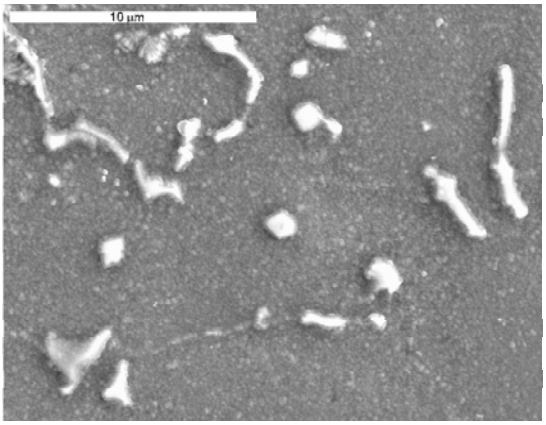

Fig. 3. Precipitates of RS carbides in FZ. Visible layer of supersaturated γ' phase solidifying on carbides or together with them. Etched with ML3. SEM – BSE

By X-ray analysis in FZ, the following three phases were identified: γ, γ' and carbides (NbTi)C. Results are shown as the X-ray spectrum in Fig. 4 and given in Table 2.

When identifying phases for the angles 2θ = 51.19; 59.72; 89.69 and 111.64, the phase Ni_3(AlTi)C was also identified, with the following interplanar distances "d" and intensities:

2θ = 51.19 d = 0.2079 nm intensity = 100 %
2θ = 59.72 d = 0.1802 nm intensity = 35 %
2θ = 89.69 d = 0.1271 nm intensity = 20 %
2θ = 111.64 d = 0.1083 nm intensity = 20 %
2θ = 119.79 d = 0.1035 nm intensity = 6 %

The phase Ni_3(AlTi)C, identified first in Inconel 100, solidifies in simple lattice Pm3m with the parameter a = 0.3589 nm [28-30]. So, parameters of this phase are close to the parameters of solid solution γ and phase γ'.

In microscopic examinations, the (NbTi)C carbides were found in FZ, surrounded by precipitates of γ' phase supersaturated with niobium. On the ground of X-ray analysis it is impossible to preclude the phase Ni_3(AlTi)C, the reflexes from which on the spectrum diagram can coincide with the reflexes from γ phase. In FZ, the carbides (NbTi)C can be present, as well as the complex phases Ni_3(AlTi)C and Ni_3(Al,Ti,Nb).

At 2θ = 97.0 as well, a reflex was observed that could be very exactly arrogated to the phase Ni_3Nb, marked often as γ", solidifying in the tetragonal system, coherent with the matrix. The interplanar distance for this angle is 0.1195 nm at the intensity of 8 %. So, it is close to the theoretical value "d" for the γ" phase of 0.1198 nm (atomic plane (123)) at the intensity of 8 %. So, it is impossible to state univocally the presence of this phase in the examined specimen. However, it is possible that aluminium in γ' phase is substituted with niobium coming mainly from the carbides (NbTi)C dis-

TABLE 2

Interpretation of X-ray diffractogram shown in Fig. 4

Measurements			Phases					
Angle 2θ	d [nm]	Intens. [%]*	Ni_3Al		NiCr-γ		(NbTi)C	
			d [nm]	Intens.	d [nm]	Intens.	d [nm]	Intens.
28.73	0.3607	13	0.3597	40				
41.30	0.2538	12	0.2545	40			0.2545	100
48.12	0.2195	8					0.2204	80
51.19	0.2072	100	0.2075	100	0.2079	100		
59.72	0.1798	45	0.1799	70	0.1799	80		
70.16	1.557	4					0.1564	43
89.69	0.1269	30			0.1271	50		
97.0	0.1195	8	–	–	–	–	–	–
111.64	0.1082	30			0.1083	80		
119.79	0.1035	29	0.1032	40				

* – The measured intensity expressed in % is related to the level of disturbances and not to the zero value in the diagram

solved during remelting. Probably, it is just the phase Ni_3(Al,Ti,Nb) that surrounds the carbide precipitates in FZ. Substitution of aluminium with niobium results in a slight change of the lattice parameter and the interplanar distances of γ' phase, so single reflexes from the planes of γ" phase can appear.

3. Methodology

The examined alloy was Inconel 713C with the following chemical composition: Cr 12.8 %, Mo 4.15 %, Nb 1.73 %, Al 6.2 %, Ti 1.04 %, C 0.12 %, B 0.017 %, Zr 5 ppm, Fe 0.19 %, Ni – remainder. The alloy was vacuum-cast in a ceramic mould in form of plates 120 x 70 x 5 mm.

The heat treatment operations were carried out on the specimen taken from the fusion zone remelted with an electron beam [17,18] and on the specimens of the base material as delivered. Heat treatment was carried out in a laboratory furnace under argon atmosphere. Three variants of heat treatment were applied, with the following parameters:

- variant I (**W1**) soaking at 1120 °C for 1 h and air-cooling + soaking at 950 °C for 4 h and air-cooling
- variant II (**W1A**) soaking at 1120 °C for 1 h and air-cooling
- variant III (**W1B**) soaking at 1120 °C for 1 h and cooling with furnace

The specimens were progressively heated up with the furnace, with a stop at 600 °C for 15 minutes. After cooling down from 1120 °C, the specimens were repeatedly heated to 950 °C with the furnace cooled before to ca. 300 °C.
The specimen remelted with an electron beam was then heat-treated according to the variant W1. The samples of the base material were subject to all the variants of heat treatment.

Metallographic examination was carried out by light and electron microscopy, using the scanning microscope JEOL JSM-5800LV-Oxford LINK ISIS-300. Polished sections for light and SEM observations were etched with ML0 (25 ml HCl, 12.5 ml HNO_3, 0.1 g $CuCl_2$, 100 ml H_2O) and electrolytically with ML_3 (100 ml H_2SO_4 (d = 1.84), 200 ml H_2O). The etching voltage was 4 to 10 V, time 10 to 60 s.

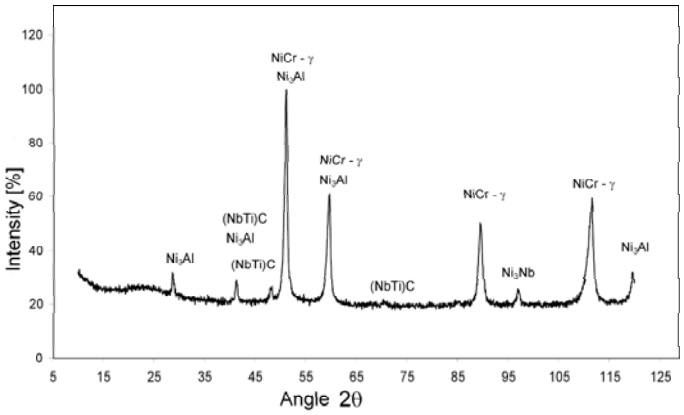

Fig. 4. X-ray spectrum of fusion zone. Radiation CoKα

4. Examination of the material melted with electron beam

On the ground of the light microscopy observations after etching with ML0 only, no differences were found between the material melted only with an electron beam and that additionally heat-treated.

In FZ after W1 treatment it was possible to observe precipitates whose colour and contrast indicated interdendritic precipitates of resolidification carbides. Morphology and arrangement of the precipitates corresponded also with the form of the RS carbides in FZ before heat treatment, see Fig. 5.

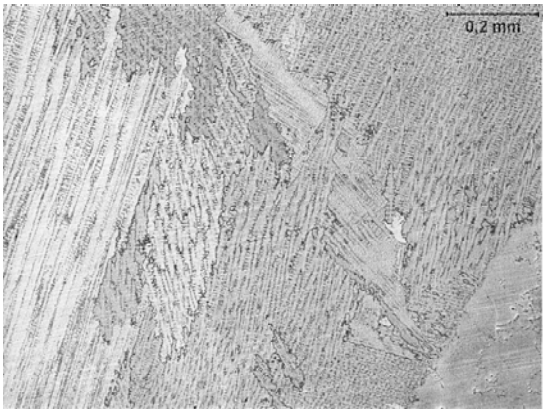

Fig. 5. Microstructure of fusion zone after heat treatment W1. Visible dark precipitates in FZ. Etched with ML0

Additional etching revealed that the observed precipitates were not RS carbides but showed a similar morphology. After etching with ML3, the precipitates in FZ were characterised by bright colour on the contrary to the primary carbides in the base material, coloured dark, see Figs. 6, 7. To compare morphology of the carbides, Fig. 7 includes a view of FZ before heat treatment.

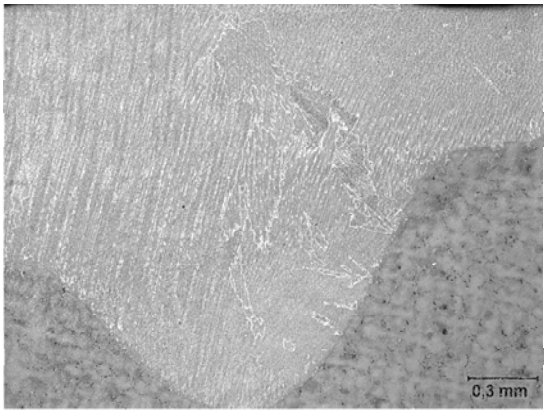

Fig. 6. Fusion zone and heat-affected zone. Visible bright precipitates in FZ and dark precipitates of primary carbides in base material. Etched with ML3

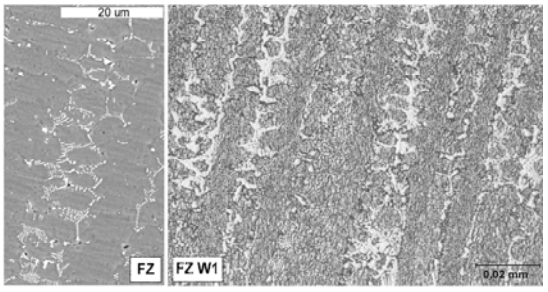

Fig. 7. FZW1: Precipitates occurring in interdendritic areas of FZ after heat treatment W1. Light microscopy. FZ: RS carbides in FZ before heat treatment. Etched with ML3. SEM – SE

The difference in colour of the carbides and precipitates indicates two separate phases differing in chemical composition or crystallographic system. During SEM observations, primary carbides were visible in the base material, but no carbides were observed in FZ. Exemplary structures of FZ, HAZ and base material are shown in Fig. 8. Shape, size and quantity of the primary carbides in the base material outside FZ did not change after heat treatment.

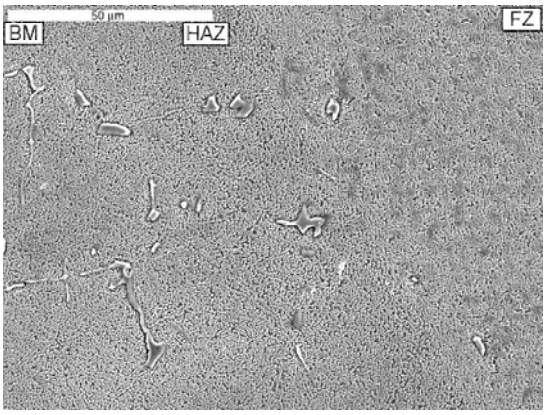

Fig. 8. Interface area of BM, HAZ and FZ. Visible primary carbides in BM and HAZ and uniform precipitates of γ' phase in the whole FZ area. Etched with ML3. SEM – SE

Bright particles in the post-carbide areas can indicate decomposition of the RS carbides in FZ and creation of a phase rich in carbon, niobium and titanium. This can be the γ' phase $Ni_3(Al,Ti,Nb)$ or the metastable tetragonal γ" phase Ni_3Nb. Dissolving of the RS carbides evidences their low stability and their decomposition already at 1120 °C. The lower decomposition temperature of the carbides can be explained by their non-equilibrum dissolution. During welding, this phenomenon proceeds faster and consists in non-equilibrum melting. In the case of heat treatment after welding, decomposition of the carbides can proceed more slowly and need not be directly related to their melting. It was found by SEM observations that the mentioned precipitates formed longitudinal, developed shapes and closed loops, see Figs. 9 to 12.

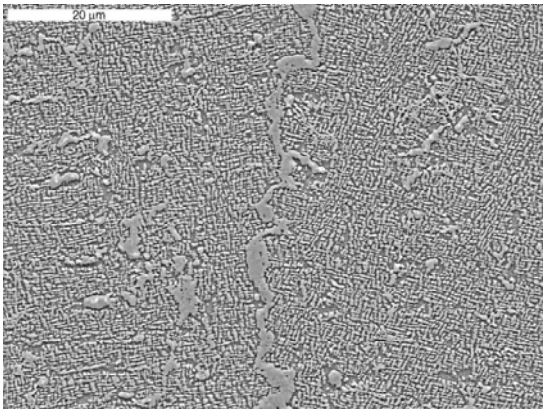

Fig. 9. Longitudinal post-carbide precipitates in FZ, globular phase γ' and austenite γ. Etched with ML3. SEM – SE

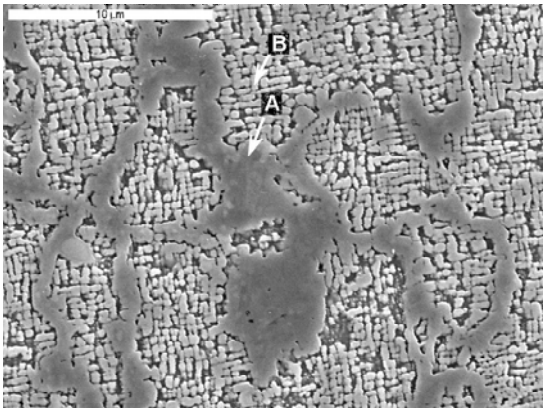

Fig. 10. Post-carbide precipitate γ' (A) and matrix γ-γ' (B) in FZ after W1. Etched with ML3. SEM – SE

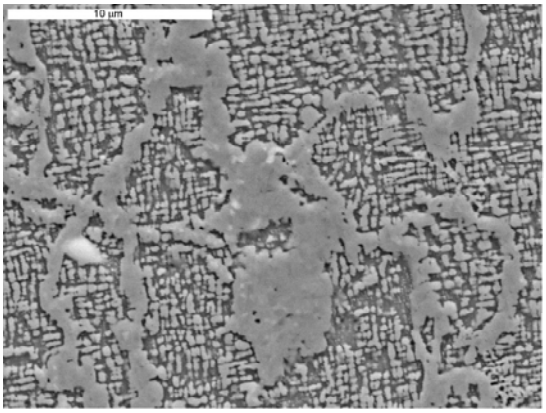

Fig. 11. The area of Fig. 10 observed using BSE detectors

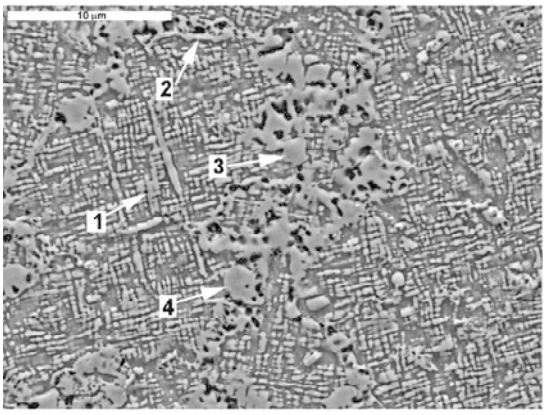

Fig. 12. Post-carbide precipitates γ' and matrix γ-γ' in FZ after W1. SEM – BSE

The precipitates are not shaped like carbides and their colour is similar to the matrix, a bit darker only. When observed under material contrast BE and BSE, their colour is similar to that of γ' phase. Fig. 11 shows the microstructure area of Fig. 10, observed under BSE.

Some small brighter points are visible in the observed precipitates, see Figs. 9 and 10, being probably residues of the dissolved RS carbides. On this ground, in this paper these precipitates are called the post-carbide precipitates.

It was found by chemical microanalysis of post-carbide precipitates as well as the matrix γ and γ' that concentration of titanium and niobium in the precipitates was ca. twice higher than in phase γ'. Concentration of molybdenum was also slightly increased. Concentration of carbon could not be determined.

These results suggest that a post-carbide precipitate is created by rebuilding a RS carbide and this is why it shows a higher content of niobium and titanium. This content is slightly higher than in the matrix, but it should be noted that the RS carbide precipitates were very tiny. Besides, niobium and titanium replace only aluminium in the phase γ'. So, most probably this is the γ' phase type Ni_3(Al,Ti,Nb). It was found in the works [31,32] that niobium carbides can precipitate from supersaturated γ solution and just from the phase Ni_3(Al,Ti,Nb). This phenomenon happens during repeatable heating after welding during operation or heat treatment. So, this phase can be supersaturated with niobium and also participate in decomposition of the precipitates.

A dozen microanalyses were made of the observed post-carbide precipitates and in many cases their composition did not significantly differ from the phase γ'. The microanalyses of the post-carbide precipitate and phase γ' of Fig. 10 are given in Table 3 in weight and atomic percentages.

TABLE 3

Chemical microanalyses of points A and B in Fig. 10 in wt% and at%

Point	**Al**	**Ti**	**Cr**	**Fe**	**Ni**	**Nb**	**Mo**
A [wt%]	6.59	1.69	15.29	0.97	64.86	5.53	5.06
A [at%]	13.50	1.95	16.26	0.96	61.11	3.29	2.91
B [wt%]	7.59	0.86	12.65	0.96	70.81	3.05	4.09
B [at%]	15.27	0.97	13.20	0.93	65.51	1.78	2.31

Microanalyses of other places also did not show any significant differences between the post-carbide phase and the γ' precipitates.

Microanalyses of the places marked 1, 3 and 4 in Fig. 12 revealed an approximate chemical composition. Results of chemical microanalysis are settled in Table 4.

In "1", the phase γ' is present with increased chromium content. It probably comes partially from the solid solution γ. Molybdenum content is also slightly increased. This difference is not significant, but can suggest that molybdenum comes from austenite γ in that is dissolved. According to some authors, molybdenum can

TABLE 4

Chemical microanalyses of points 1, 2, 3 and 4 in Fig. 12 in at%

Point	Al	Ti	Cr	Fe	Ni	Nb	Mo
1	16.57	1.12	10.67	1.39	66.23	1.47	2.52
2	13.13	2.10	17.52	0.90	57.90	5.11	3.30
3	18.07	1.22	6.17	1.09	70.25	1.54	1.62
4	17.21	2.03	4.69	0.67	72.13	2.28	0.96

be also present in γ' phase, replacing aluminium [9]. Aluminium and nickel contents in the places 1, 3 and 4 are similar, but chromium content in the precipitates 3 and 4 is clearly lower. This indicates that these precipitates are thicker and chromium from austenite γ' affects the results to a smaller degree. However, it can not be univocally stated that it does not come from a precipitate, since it can be present in the RS carbides and can participate in the reaction of rebuilding the carbides into the phase γ'.

Types of the phases can not be univocally determined on the ground of the EDX analysis. However, comparison of the results of numerous analyses permitted determining the ratio of concentration of nickel to total concentration of (Al+Ti+Nb+Mo) at the places 1, 3 and 4 in Fig. 12 and A and B in Fig. 10. The calculated value should be treated as an approximate value only, but it is very close to 3/1 resulting from the stoichiometric formula of Ni_3(Al,Ti) and namely is 3.2/1 in the point 1; 3.1/1 in the point 3 and 3.2/1 in the point 4. Chromium and iron were omitted in the calculations.

In the phase marked A in Fig. 10, the concentration ratio is 2.8/1 and in the phase marked B it is 3.2/1. It should be noted that, in spite of many factors influencing the chemical microanalysis, the calculated values of Ni/(Al,Ti,Nb,Mo) show a high consistence. In the phase marked 2 in Fig. 12, the concentration ratio is 2.4/1. So, the difference is larger and proves slower decomposition of the carbide that has not been yet rebuilt to the phase γ'.

Decomposition of the RS carbides occurs in diffusive way, which is proved by bright microareas inside the precipitates. The new post-carbide phase Ni_3(AlTiNb) is first created probably by annexing the atoms of nickel and aluminium coming from austenite γ to carbides. It can also grow by incorporation and coalescence of γ' particles, this way evening the chemical composition.

The reaction formulae mentioned in literature [1,5,12] do not consider the possibility that carbides are not created, and such a phenomenon occurred in the heat-treated fusion zone. So, a reaction must happen in that carbon dissolves in the γ solution (the introduced notation γC) or creates the new phase Ni_3(Al,Ti,Nb,Mo)C denoted as γ'C, whose presence in the alloy was suggested in the X-ray examinations. So, the applied formulae should be modified as follows:

$$\begin{gathered} MC + \gamma = \gamma' + (\gamma C) \\ (Nb, Mo, Ti)C + (Ni, Cr, Al, Ti) = Ni_3(Al, Nb, Ti, Mo) + (Ni, Cr, Al, Ti, Mo, C) \end{gathered} \quad ([1])$$

$$\begin{gathered} MC + \gamma = (\gamma' C) + \gamma \\ (Nb, Mo, Ti)C + (Ni, Cr, Al, Ti) = Ni_3(Al, Ti, Nb, Mo)C + (Ni, Cr, Al, Ti, Mo) \end{gathered} \quad ([2])$$

$$\begin{gathered} MC + \gamma = (\gamma' C) + \gamma' \\ (Nb, Mo, Ti)C + (Ni, Cr, Al, Ti) = Ni_3(Al, Ti, Nb, Mo)C + Ni_3(AlTi) \end{gathered} \quad ([3])$$

$$\begin{gathered} MC + \gamma \rightarrow (\gamma' C) \rightarrow \gamma' + (\gamma C) \\ (Nb, Mo, Ti)C + (Ni, Cr, Al, Ti) = Ni_3(Al, Ti, Nb, Mo)C \rightarrow Ni_3(Al, Ti, Nb) + (Ni, Cr, Al, Ti, Mo, C) \end{gathered} \quad ([4])$$

The fourth formula is the most general. The performed observations suggest that the carbides can decompose in this sequence. Unfortunately, it is impossible to determine distribution and concentration of carbon, but it seems that the phase Ni_3(Al,Ti)C will not be stable and after longer soaking will be rebuilt to γ', and carbon will dissolve in austenite. Solubility of carbon in nickel at 1100 °C is high, amounting to ca. 2.5 % [15].

5. Microanalysis of Inconel 713C after heat treatment

As a result of heat treatments W1 and W1B, local eutectic areas ($\gamma - \gamma$')-(M_xC_y) were found on grain boundaries. In addition, precipitates on the boundary were pre-melted. In the base material before heat treatment, the eutectic areas ($\gamma - \gamma$') were only observed, occurring locally inside the grains. The developed eutectic areas are shown in Figs. 13 and 14. The heat treatment W1A caused only coagulation and coalescence of γ' particles in the areas of grain boundaries and the primary carbides (NbTi)C precipitated on them. This is related to short soaking time and fast cooling.

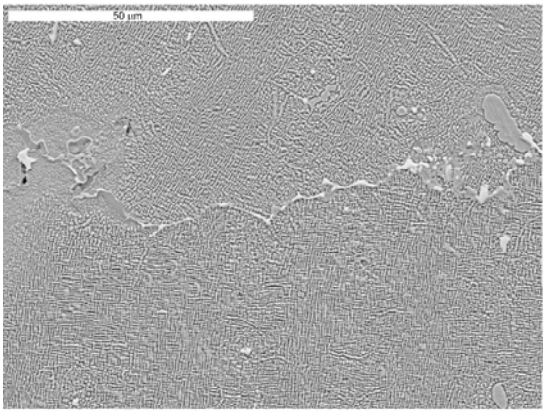

Fig. 13. Grain boundary in base material after heat treatment W1B. Melted grain boundary and eutectic particles MC-γ-γ'. Etched with ML3. SEM – SE

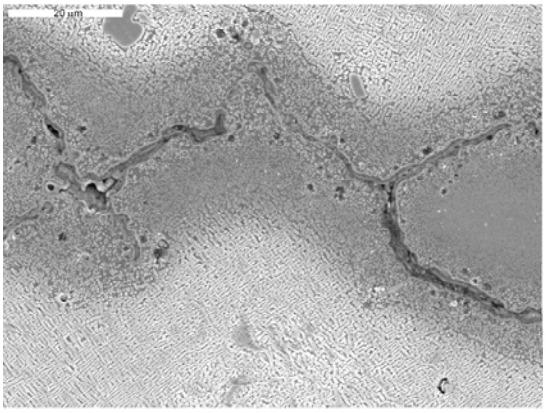

Fig. 14. Magnified view of grain boundary shown in Fig. 13. Morphology of the grain boundary indicates melting of the phases located on it. Etched with ML3. SEM – SE

Microanalysis of eutectic areas revealed the presence of both the carbides (NbTi)C and $(Cr,Mo,Nb,Ti)_{23}C_6$ or M_6C. Two microanalyses of the carbide precipitates in the specimens W1 and W1B revealed also zirconium content of ca. 10 and 22 wt%, as well as a small, 5% content of silicon. This evidences segregation of zirconium to the eutectic MC-γ-γ', which additionally lowers its solidification point below 1120 °C. In the works of Ojo, Lippold, Huaxin and others [24,33,34], solidification point of the zirconium-rich eutectic mixtures type Ni-Zr_{15}(Ni,Al,Cr)$_{85}$ was 1175 °C. On the other hand, annealing at 1100 °C for 23 h resulted in decay of eutectic areas in the base material. The heat treatment described in this work resulted in melting the zirconium-rich eutectic MC-γ-γ' at the temperatures below 1120 °C, which are also lower than the temperature mentioned in [24,33,34]. The additional presence of silicon can indicate creation of low-melting precipitates type NbSi on the carbides containing niobium or decomposition of the carbides NbC.

In the base material, on some carbide precipitates an envelope of the phase γ' was also observed, that precipitated on them and could participate in their decomposition. Exemplary precipitates of carbides are visible in Fig. 15. Similar precipitates were also found in fusion zones, see Fig. 3. Shape and broadening of edges of the carbides, as well as coagulation of γ' particles around the carbides, found in the specimens W1, W1A and W1B, indicate that they were subject to decomposition at 1120 °C in diffusion way. These carbides in the base material did not decay completely because they were relatively large and the annealing time was short.

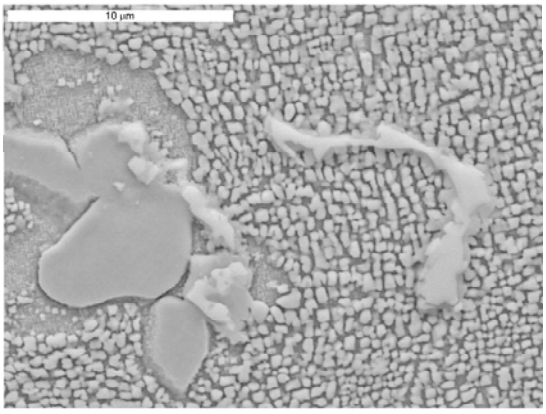

Fig. 15. Eutectic mixture MC-γ-γ' in the specimen W1. Visible layer of the phase Ni_3(Al,Ti,Nb) precipitated on carbides. Etched with ML3. SEM – SE

So, the supersaturated phases γ' – Ni_3(Al,Ti,Nb) or Ni_3(Al,Ti,Nb)C surrounding the carbides (NbTi)C can participate in their decomposition. A possibility should be also accepted that the eutectic mixture (NbTi)C-γ' or (NbTi)C-(γ-γ') is created, what is indicated by melted areas of the microstructure. Therefore, decomposition of the carbides can occur by local reaching eutectic chemical composition on the interface carbide-matrix. Thus, this is a phenomenon close to the non-equilibrium melting. Like this, another model of decomposition of the MC carbides should be also considered, obtained by introducing a correction to the formula 4:

$$MC + \gamma \rightarrow (MC - \gamma') \rightarrow \gamma' + (\gamma C)$$
$$(Nb, Mo, Ti)C + (Ni, Cr, Al, Ti) = [(Nb, Mo, Ti)C - Ni_3(Al, Ti)] \rightarrow Ni_3(Al, Ti, Nb) \quad ([5])$$
$$+(Ni, Cr, Al, Ti, Mo, C)$$

or

$$MC + \gamma \rightarrow (MC - \gamma - \gamma') \rightarrow \gamma' + (\gamma C)$$
$$(Nb, Mo, Ti)C + (Ni, Cr, Al, Ti) = [(Nb, Mo, Ti)C - Ni_3(Al, Ti) - (Ni, Cr, Al)] \rightarrow Ni_3(Al, Ti, Nb) \quad ([6])$$
$$+(Ni, Cr, Al, Ti, Mo, C)$$

6. Conclusions

1. Decomposition of the carbides (NbTi)C need not proceed through creation of the complex carbides $M_{23}C_6$ or M_6C.
2. The carbides (NbTi)C are not stable to the temperature 1180 °C and can decay after a short time of soaking at 1120 °C.
3. Heat treatment of fusion zones results in complete decay of carbides and to creation of the phase Ni3(Al,Ti,Nb) supersaturated with niobium, austenite γ supersaturated with carbon or the phase Ni_3(Al,Ti,Nb)C.
4. Heat treatment of base material also results in local decay of the carbides (NbTi)C. Decomposition of the carbides can occur by non-equilibrium reaching the eutectic composition of (NbTi)C-($\gamma - \gamma$') and next creating the phase Ni_3(Al,Ti,Nb) and austenite γ supersaturated with carbon.

Acknowledgements

This scientific work was financed by Wroclaw University of Technology from the science funds in the years 2007/2008 as a research project No. 332697.

REFERENCES

[1] B. Mikułowski, Heat-resisting and creep-resisting alloys – superalloys; AGH 27-54, (1997) (in Polish).
[2] E. O. Ezugwu, Z. M. Wang, A. R. Machado, Mater Prog Tech **86** 1-16 (1999).
[3] H. K. D. H. Bhadeshia, Nickel Based Superalloy. www.msm.cam.ac.uk/phase-trans/2003/superalloys/superalloys.html.
[4] C. P. Sullivan, M. J. Donachie, F. R. Morral, Cobalt-base superalloys-1970, Centre d'information du cobalt; Brussels (1970).
[5] W. R. Sun, J. H. Lee, S. M. Seo, S. J. Cheo, Z. Q. Hu, Mat. Sci. Eng. **A271**, 143-149 (1999).
[6] F. Zupanič, T. Bončina, A. Križman, F. D. Tichelaar, J Alloys Compo **329**, 290-297 (2001).
[7] T. Bončina, F. Zupanič, A. Križman, B. Markoli, S. Spaič, Pract Metallog **41**, 373-385 (2004).
[8] T. J. Garosshen, T. D. Tillman, G. P. McCarthy, Metall Trans **18A**, 69-77 (1987).
[9] A. Czyrska-Filemonowicz, The influence of helium on the structure of nickel-base alloys; Wyd. PAN, 23-94 (1989), (in Polish).
[10] F. S. Yin, X. F. Sun, J. G. Li, H. R. Guan, Z. Q. Hu Z, Scripta Mater **48**, 425-429 (2003).
[11] J. Chen, J. H. Lee, C. Y. Jo, S. J. Choe, Y. T. Lee, Mat Sci Eng **A 247**, 113-125 (1998).
[12] F. M. Yang, X. F. Sun, W. Zhang, Y. P. Kang, H. R. Guan, Z. Q. Hu, Mater Latt **49**, 160-164 (2001).
[13] J. Szala, A. Szczotok, J. Richter, J. Cwajna, A. Maciejny, Mater Charact **56**, 325-335 (2006).
[14] A. Szczotok, J. Szala, J. Cwajna, M. Hetmańczyk, Mater Charact **56**, 348-354 (2006).
[15] M. Hansen, Constitution of binary alloys; McGraw-Hill Book Company INC. New York (1958).
[16] W. H. Jiang, X. D. Yao, H. R. Guan, Z. Q. Hu, Metall Mater Trans **30A**, 513-517 (1999).
[17] M. Lachowicz, W. Dudziński, K. Haimann, M. Podrez-Radziszewska, Mat Sci Eng **A 479**, 269-276 (2008).
[18] M. Lachowicz, W. Dudziński, K. M. Podrez-Radziszewska, Mater Charact **59**, 560-566 (2008).
[19] M. Qian, J. C. Lippold, Weld Jour, 145-150 (June 2003).
[20] W. Chen, M. C. Chaturvedi, N. L. Richards, G. McMahon, Metall Mater Trans **29A**, 1947-1954 (1998).
[21] W. Chen, M. C. Chaturvedi, N. L. Richards, Metall Mater Trans **32A**, 931-939 (2001).
[22] O. A. Ojo, M. C. Chaturvedi, Mat Sci Eng **A 403**, 77-86 (2005).
[23] O. A. Ojo, N. L. Richards, M. C. Chaturvedi, Scripta Mater **50**, 641-646 (2004).
[24] O. A. Ojo, N. L. Richards, M. C. Chaturvedi, Scripta Mater **51**, 683-688 (2004).
[25] O. A. Ojo, N. L. Richards, M. C. Chaturvedi, Scripta Mater **51**, 141-146 (2004).
[26] C. Huang, S. Kou, Weld Reseach **5**, 113-120 (2000).

[27] ASM Handbooks on-line, www.products.asminternational.org/hbk/index.jsp.
[28] W. B. Pearson, A handbook of lattice spacings and structures of metals and alloys vol. 2; Pergamon Press, London (1967).
[29] P. Villars, L. D. Calvert, Pearson's handbook of crystallographic data for intermetallic phases vol. 1,2,3; American Society for Metals, (1985).
[30] International Centre for Diffraction Data ICDD; USA (1996).
[31] A. J. Ramirez, J. C. Lippold, Mat Sci Eng **A 380**, 259-271 (2004).
[32] A. J. Ramirez, J. C. Lippold, Mat Sci Eng **A 380**, 245-258 (2004).
[33] L. Huaxin, R. H. Jones, Mat Sci Eng **A 192/193**, 563-569 (1995).
[34] L. Huaxin, T. K. Chaki, Mat Sci Eng **A 192/193**, 571-576, (1995).

Received: 10 October 2009.